Optimum Radio Resource Management in Carrier Aggregation based LTE-Advanced Systems

Soheil Rostami, Kamran Arshad, *Senior Member, IEEE,* and Predrag Rapajic, *Senior Member, IEEE*

***Abstract*—Carrier Aggregation (CA) functionality introduces new challenges for Radio Resource Management (RRM) function of network. In this article, an optimum and efficient RRM algorithm is proposed for Long Term Evolution-Advanced (LTE-A) with reduced complexity and compared with the State-Of-The-Art (SOTA) solutions. The proposed algorithm optimally assigns Component Carriers (CCs), Resource Blocks (RBs) and Modulation and Coding Scheme (MCS) values to users, based on their Channel State Information (CSI) and CA capabilities. Most of the SOTA solutions are based on approximate approaches which have much inferior performance compared to the performance of our proposed optimal solution. Furthermore, performance of the proposed solution has been evaluated using system-level simulations, and results show clearly that the proposed algorithm outperforms the SOTA algorithms in terms of fairness throughput and average cell throughput.**

***Index Terms*—carrier aggregation, resource allocation, link adaptation, scheduling, radio resource management**

I. Introduction

In order to satisfy exponential growth of wireless data services and growing number of wireless users, International Telecommunication Union (ITU) initiated a global standard - which is referred to as International Mobile Telecommunications-Advanced (IMT-A) or Fourth-Generation mobile systems (4G) - to identify an all-IP cellular network whose capabilities go beyond those of IMT-2000 [1], [2]. Specific requirements for IMT-A have been set to minimum support of 40 MHz bandwidth, 1 Gbps and 500 Mbps peak data rates for Down Link (DL) and Up Link (UL) respectively [1], [2], [3], [4], [5].

Since 2004, 3rd Generation Partnership Project (3GPP) has been developing LTE, and the first complete set of specifications (i.e. Release 8 - Rel-8) was published in 2008, providing DL and UL peak data rates up to 300 Mbps and 75 Mbps respectively. In response to ITU invitation for the submission of potential technologies for IMT-A, 3GPP started LTE-A specifications in 2008, and published Rel-10 in 2010; later in the same year, ITU approved LTE Rel-10 (LTE-A) as one of two IMT-A technologies. LTE-A not only fulfils IMT-A requirements, but in many cases even surpasses them [6]. LTE-A provides a suitable base for enhanced services because of the provision of higher data rates, improved coverage and lower latency services [7]. To achieve ITU aggressive performance targets, LTE-A 1) improves spectrum flexibility by introducing CA, 2) enhances Multiple-Input Multiple-Output (MIMO) technology by supporting up to eight transmission layers in DL, 3) extends coverage, and provides support to cell-edge users by introducing relay nodes, and 4) enables interference management between different power class cells as well as open access and closed subscriber group cells [8].

To support peak data rates of up to 1 Gbps, the use of high channel bandwidth is imperative. However, worldwide Mobile Network Operators (MNOs) do not have access to a continuous segment of wide bandwidth (e.g. 100 MHz) due to the spectrum fragmentation [9]. To achieve this, 3GPP introduced CA as one of the most important features in Rel-10, and subsequently enhanced in Rel-11 and Rel-12. CA allows efficient and flexible usage of fragmented spectrum by aggregating up to five CCs each with bandwidth of up to 20 MHz. This allows an overall transmission bandwidth of up to 100 MHz, and correspondingly higher data rates of up to 1 Gbps [10].

This article is organised as follows. The RRM functionality of LTE-A is concisely reviewed in Section II. A brief summary of related works is presented in Section III. In Section IV, a joint RRM problem is formulated as an optimisation problem. The proposed solution is explained in Section V, and proof of optimality of the solution is given in Appendix. Computational complexity analysis and simulation results are discussed in Section VI and VII respectively, followed by conclusions in Section VIII.

II. Background Review

To achieve high spectral efficiency and peak data rates, Orthogonal Frequency Division Multiplexing (OFDM) with a shared channel concept for DL data transmission is adopted in LTE [11], [12]. A RB is defined as N_s consecutive OFDM symbols in the time domain and N_{sc} consecutive subcarriers in the frequency domain [12]. Moreover, a RB occupies exactly one time slot with duration of 0.5 ms, and corresponds to bandwidth of 180 KHz. A RB is the smallest radio resource that LTE applies for allocating spectrum every double-time slots - which is referred to as Transmission Time Interval (TTI). Tables 3.1.1-1 and 3.1.1-2 in [13] depict RB parameters defined in LTE for different settings. According to 3GPP TR 36.912 [4], LTE supports only CC configuration with bandwidth equals $\{1.4, 3, 5, 10, 15, 20\}$ MHz, and their corresponding number of RBs $\{6, 15, 25, 50, 75, 100\}$.

In LTE, to compensate for the instantaneous radio-link conditions, and to make efficient use of the channel capacity,

S.Rostami and P.Rapajic are with Department of Engineering Science, University of Greenwich, U.K. E-mail: {S.Rostami, P.Rapajic}@gre.ac.uk.

K.Arshad is with Department of Electrical Engineering, Ajman University, UAE. E-mail: K.Arshad@ajman.ac.ae.

link adaptation by means of Adaptive Modulation and Coding (AMC) is employed. In AMC, the radio-link data rate is controlled by adjusting MCS-index value - which is referred to as k. For instance, if Signal-to-Noise Ratio (SNR) for radio-link is sufficiently high, higher order modulation with higher code rate can be used to increase capacity. Furthermore, let R_k be the code rate associated with k, M_k be the constellation size of k, and t_s be the time-slot duration, data rate $d(k)$ achieved by k for a single RB can be obtained from $d(k) = (1/t_s)\, R_k \log_2 (M_k)\, N_{sc} N_s$.

To select an appropriate MCS for DL transmission, User Equipment (UE) provides CSI to evolved Node B (eNB), indicating the instantaneous DL channel quality in both time and frequency domains. The contents of CSI in the absence of MIMO consists of only Channel Quality Indicator (CQI), and can be obtained by measuring SNR on the reference signals transmitted in DL [12]. The value of CQI-index value per RB, implicitly indicates the maximum data rate that a UE can achieve with a Block Error Rate (BLER) of 10% or below on the RB [14].

According to 3GPP TS 36.213 [15], there are 16 different CQI index values (4 bits) ranging from 0 to 15; where 0 and 15 indicate the out of range and best channel quality respectively. Corresponding modulation scheme, code rate and data rate per RB can be obtained from Table 7.2.3-1 in [15]. In this article, the method mentioned in [14] is adopted to map CQI index values to their corresponding SNR values (and vice versa). Based on CQI values, the highest-rate k per CC per UE in a given TTI is assigned.

As mentioned in Section I, CA enables MNOs to create large virtual carrier bandwidth for data hungry users by aggregating multiple CCs with different bandwidth, dispersed within intra or inter bands [10], [16]. In addition to enabling higher transmission bandwidth, simultaneous utilisation of RBs across multiple CCs offers an extra frequency diversity due to the fact that assigned CCs experience different propagation conditions which affect achievable data rates [10].

LTE-A UE has one DL Primary Component Carrier (PCC) and an associated UL PCC. Also, it may have one or several Secondary Component Carriers (SCCs) in either DL or UL direction in the licensed or unlicensed spectrum [17], [18]. Similar to LTE UE, the configuration of PCC is UE-specific [19], [20]. When a UE with CA capability starts establishing or re-establishing Radio Resource Control (RRC) connection with eNB (using cell search and random access procedures), following the same steps as in the absence of CA, only PCC is configured. Once the communication between eNB and UE is established, additional SCCs can be configured by RRM functionality located at eNB. In other words SCC assignment is cell-specific, and signalled as part of the system information [19], [20].

The RRM functionality plays an important role in optimising network performance from an operator perspective, as well as improving Quality of Service (QoS) of users [21]. It exploits various functionalities, including QoS management, admission control, hybrid automatic retransmission request, link adaptation, and resource scheduling [22], [23]. The RRM for LTE-A has many similarities with that of LTE except modification of resource scheduling and inclusion of a new functionality known as SCC selection. This functionality configures SCC sets for each UE with CA capability in both UL and DL directions. The resource scheduler assigns RBs within cell-selected SCCs and UE-selected PCCs. In other words, LTE UEs benefit from dynamic scheduling of RRM only within PCCs, while LTE-A UEs not only take advantage of PCCs but also SCCs. Resource allocation strategy is not specified by 3GPP and is operator-specific [19], [24].

III. Related Works, Contributions, Assumptions and Notations

A. Related Works

Since LTE-A, concept of RRM for CA-enabled LTE networks has gained significant attention [10], [25], [26]. Most of the previous studies related to RRM in LTE-A, assumed CC selection, RB allocation and MCS assignment as completely separate problems which consequently lead to the degradation of network performance. For instance, Tian *et al.* [27] developed a RRM algorithm that assigns CCs to each newly-arrived UE on the basis of the average channel quality, independent of RB allocation. In [28], CC selection and RB allocation were considered jointly, but link adaptation (MCS assignment) was neglected. Wu *et al.* [28] proposed a Minimising System Utility Loss (MSUL) algorithm, in which UEs can be categorised either as narrow-band or broadband where the former can support only one CC while the latter can support all CCs in a given cell [28]. The MSUL algorithm assigns each CC independently, and after assigning all CCs, the algorithm removes least-contributed CCs (except one CC) to the utility function from narrow-band UEs.

More recently, Liao *et al.* [25] proposed a radio resource allocation scheme, and referred to it as Greedy Algorithm (GA). The GA considered MCS assignment jointly with CC selection and RB allocation. The authors assumed that all CCs have the same number of RBs, and all UEs have the same CA capability, however both assumptions are unrealistic. Moreover, GA is an iterative process that calculates the utility function for all possible combinations of UEs, CCs and MCSs at each iteration. An assignment with the highest value of the utility function is selected at each iteration until the algorithm converges [25].

Most of the current research neglected LTE-A constraints in respect to PCC and SCC selections. Further, all of the mentioned SOTA solutions did not optimise RRM functionality, and are based on approximate algorithms that only achieve half of the Proportional Fair (PF) objective function of the optimal solution. TABLE I briefly explains some of the SOTA solutions available in literature, and compares them with the proposed algorithm in this article - Optimum Resource block Allocation Algorithm (ORAA).

B. Contributions

The core RRM strategy presented in this article is to take advantage of multiuser diversity in both time and frequency dimensions across different CCs (multicarrier diversity), and schedule transmissions to UEs on RBs with better channel

TABLE I: Recent RRM methods for CA-enabled LTE-A networks available in literature

References	Characteristics	Advantages	Disadvantages	MCS Constraint	SCC Assignment	Power Allocation	QoS	MIMO
[27]	A novel CC selection method is proposed	An improvement on the performance of network for non-continuous CA with low complexity	RB allocation and CC allocation are considered independently	✗	✗	✗	✗	✗
[28]	CC selection and RB allocation are considered jointly	Improving system performance compared with the SOTA methods	Based on an iterative process	✗	✗	✗	✗	✗
[25] [29]	MCS assignment is considered jointly with CC selection and RB allocation	Guaranteeing at least half of the performance of the optimal solution	Based on an iterative process	✓	✗	✗	✗	✗
[20]	Energy-efficient CA algorithms are proposed	Guaranteeing performance under various models of continuous and non-continuous CA as well as backlogged and finite user buffers	Based on an approximation approach	✓	✓	✓	✗	✗
[30]	Joint CA and packet scheduling method considering packets delay is introduced	Achieving load balancing across CCs, better throughput and delay performance for users compared with the existing schemes	A two-tier resource allocation framework which incorporates dynamic CC assignment and backlog-based scheduling schemes	✓	✗	✗	✓	✗
[31]	Joint CA and packet scheduling for LTE with MIMO is investigated	Considering MIMO mode selection based on users mobility	Based on greedy algorithm	✓	✗	✗	✗	✓
ORAA	Joint CA and RB allocation for LTE systems is studied	An optimal and efficient solution	Did not consider MIMO mode selection and QoS requirements of users	✓	✓	✗	✗	✗

conditions. In addition, designing a high performance low-complexity RRM framework is vital, due to the fact that mentioned functions are highly dynamic, and new decisions have to be made in each TTI. To address these issues, an optimum and efficient LTE-compliant solution for RRM using PF scheduling is proposed. The major contributions of this article are threefold:

1) A joint optimisation problem to maximise PF objective function in LTE-A networks is formulated, considering RRM functionality with CA, MCS assignment, SCC selection and RB allocation. The proposed formulation considers MCS constraint as specified in 3GPP TR 36.912 [4], which requires only one MCS to be selected for each assigned CC across all its assigned RBs for a UE at any TTI in the absence of MIMO spatial multiplexing.
2) The resultant optimisation problem is shown to belong to a class of intractable Integer Linear Programming (ILP). It is proven that solving the equivalent Linear Programming (LP), using theory of total unimodular matrices, provides the same result as solving the ILP, that leads to an efficient approach for RRM. The worst-case complexity analysis is provided, and clearly verifies ORAA's computational efficiency.
3) The extensive system-level simulations are performed to validate performance of the proposed solution, and to compare it with GA [25].

To the best of authors' knowledge, this work is the first attempt to propose an LTE-compliant optimal joint allocation of RBs, SCCs and MCSs. Most of the existing research either solve the allocation problem in non-CA based LTE systems [32], [33], [34], or by solving the problem in CA-based LTE systems, using greedy algorithms which guarantee only half of the optimum PF criterion [25], [26], [29].

C. Assumptions

1) In LTE for DL transmission, eNB distributes its power budget to RBs according to their corresponding channel qualities. For near-optimal power allocation, the water-filling approach could be used whereby higher power is allocated to subcarriers whose fading and interference are in favourable conditions [35]. However, Yu *et al.* [36] proved that for the Rayleigh fading channel in an adaptive modulation framework, spectral efficiency loss due to constant-power water-filling is negligible. Hence, in this article for simplicity purposes, it is assumed that DL power is distributed uniformly over RBs, i.e. no DL power control is employed.
2) The set of RBs, SCCs and MCSs are allocated for next scheduling time slot based on UEs measurements

in previous CQI reports. Therefore, predictability of channel conditions has high importance from the overall system point of view; large and uncorrelated interference variation or high mobility of UEs from one time slot to the other makes the network optimisation difficult. In this article, CQI feedback is assumed to vary slowly in each scheduling time slot, and is available on a RB size granularity over all CCs.

3) To assess network performance, the backlogged traffic model (known as full-buffer model) is used where queue length of every UE is much longer than what can be scheduled during each TTI [25].
4) The proposed formulation does not consider buffer size of UEs, as well as QoS class identifier of packets - which is a method to ensure bearer traffic is allocated appropriate QoS. Therefore, different types of bearer traffic are treated as one.
5) There are a number of methods available for PCC selection [37]; in this study, UEs select their corresponding PCCs based on Reference Signal Received Power (RSRP) of the candidate CCs; i.e. CC with the highest RSRP is selected as a PCC by each UE. The RSRP is obtained as result of linear average of the DL cell-specific reference signals across the channel bandwidth.

D. Mathematical Notations

This section presents notations that are commonly used in equations throughout the following sections. In this article, vectors of dimension n are denoted by small bold letters (e.g. $\mathbf{x}_n$), and matrices are denoted by capital letters (e.g. C). Hence, $\mathbf{0}_n$ denotes the n-component all-zero vector, and $\mathbf{1}_n$ denotes the n-component all-one vector. Occasionally vector subscripts can be removed to save space, in that case, the exact vector size can be realised from the context. Further, I_n represents the $n \times n$ identity matrix, and $(.)^T$ denotes the transpose operation. A block diagonal matrix, $A = blkd(B, b)$ represents matrix of the form:

$$A = \begin{bmatrix} B & 0 & \dots & 0 \\ 0 & B & \dots & 0 \\ \vdots & \vdots & \ddots & \vdots \\ 0 & 0 & \dots & B \end{bmatrix}$$

where 0 is an all-zero matrix with the same size as B which is repeated b times.

Notation $\mathbf{x}_n \preceq \mathbf{y}_n$ for vectors $\mathbf{x}_n$ and $\mathbf{y}_n$ means that the inequality holds in each component. Furthermore, $x^{(t)}$ represents the amount of variable x at t^{th} TTI. Additionally, $C^{(n)}$ refers the outcome matrix of n^{th} step's operation over $C^{(n-1)}$ (in case of $n = 1$, $C^{(1)}$ is obtained from an operation on C). Finally, $\mathcal{O}(.)$ - is known as big O notation - describes the limiting behavior of a function when its argument tends towards infinity.

IV. SYSTEM MODEL AND PROBLEM FORMULATION

A. System Model Definition

In this work, an LTE-A cell, consisting of N UEs as $\mathcal{N} = \{1, 2, \cdots, N\}$, is considered. Each UE may have different CA capability (representing maximum number of CCs that the given UE can support) which is modelled as μ_n, for instance, if n^{th} UE is a Rel-8 UE, $\mu_n = 1$. According to the Rel-10 and beyond, UE may aggregate maximum 5 CCs (i.e. $\mu_n \in \{1, 2, ..., 5\}$).

All UEs in a given TTI, compete for M non-overlapping orthogonal CCs as $\mathcal{M} = \{1, 2, \cdots, M\}$ where each CC has a different number of RBs, and can be written as γ_m where $\gamma_m \in \{6, 15, 25, 50, 75, 100\}$ is the number of RBs in the m^{th} CC. In the absence of multiuser MIMO, each scheduled UE utilises a number of RBs and multiple CCs simultaneously while each RB is assigned exclusively to one UE at any time.

Furthermore, each CC can be chosen as a PCC or SCC for different UEs, i.e. a certain CC for a specific UE can be selected as a PCC, but same CC can be selected as a SCC for another UE. CQI-index value of n^{th} UE in p^{th} RB of m^{th} CC is represented by $c_{m,p,n} \in \mathcal{K} = \{0, 1, ..., K\}$, $\forall m \in \mathcal{M}$, $\forall n \in \mathcal{N}$ and $\forall p \in \mathcal{P} = \{1, 2, ..., P\}$ where K and P are 15 and the maximum of γ_m respectively.

To represent RB allocation, a binary variable $a^k_{m,p,n}$ is also defined where $m \in \mathcal{M}$, $n \in \mathcal{N}$, $p \in \mathcal{P}$ and $k \in \mathcal{K}$. The value of $a^k_{m,p,n} = 1$ if and only if p^{th} RB located in m^{th} CC is allocated to n^{th} UE with k as a MCS-index value and for $a^k_{m,p,n} = 0$, otherwise. A binary variable $e^k_{m,n}$ is defined to represent CC (PCC and SCC) allocation, where $e^k_{m,n} = 1$ represents m^{th} CC is assigned to n^{th} UE with k as a MCS-index value, and for $e^k_{m,n} = 0$, otherwise. Finally, to represent PCC allocation for each UE, another binary variable $y_{m,n}$ is defined where $y_{m,n} = 1$ represents m^{th} CC is selected by n^{th} UE as its PCC, and for $y_{m,n} = 0$, otherwise.

Both $a^k_{m,p,n}$ and $e^k_{m,n}$ must satisfy following conditions:

1) The interference constraint defined in (1) must be satisfied, i.e. two or more UEs cannot utilise the same RB simultaneously. In addition, (1) ensures that there is maximum one non-zero k per allocated RB:

$$\sum_{n=1}^{N} \sum_{k=1}^{K} a^k_{m,p,n} \leq 1 \tag{1}$$

2) CA capability of each UE must be taken into account, i.e. number of aggregated CCs for each UE should be less than its maximum supported aggregating CCs:

$$\sum_{m=1}^{M} \sum_{k=1}^{K} e^k_{m,n} \leq \mu_n \tag{2}$$

3) p^{th} RB located in m^{th} CC is allocated to n^{th} UE with k as a MCS-index value ($a^k_{m,p,n} = 1$), if m^{th} CC is allocated to n^{th} UE with k as a MCS-index value ($e^k_{m,n} = 1$), i.e.

$$a^k_{m,p,n} \leq e^k_{m,n} \tag{3}$$

4) All allocated RBs to n^{th} UE in m^{th} CC must have identical k (MCS constraint), i.e.

$$\sum_{k=1}^{K} e^k_{m,n} \leq 1 \tag{4}$$

5) Because each UE has one and only one PCC, in case that m^{th} CC is selected as a PCC for n^{th} UE ($y_{m,n} = 1$), there is a k where $e^k_{m,n} = 1$, i.e.

$$y_{m,n} \leq \sum_{k=1}^{K} e^k_{m,n} \tag{5}$$

For n^{th} UE, achievable throughput (f_n) can be estimated as follows:

$$f_n = \sum_{m=1}^{M}\sum_{p=1}^{P}\sum_{k=1}^{K} r^k_{m,p,n} a^k_{m,p,n} \tag{6}$$

where

$$r^k_{m,p,n} = \begin{cases} 0 & \text{for } c_{m,n,p} < k \\ d(k) & \text{for } c_{m,n,p} \geq k \end{cases} \tag{7}$$

In 3GPP LTE standard, all RBs allocated to a given UE per CC must adopt the identical MCS, therefore it is vital that only those RBs that can provide the required QoS (BLER $\leq 10\%$) are selected [19], [25]. For this reason, (7) ensures that if a RB's CQI is lower than target MCS, then the RB cannot be utilised to transmit data by the MCS.

The original PF scheduling aims to maximise the logarithmic utility function $\sum_{n=1}^{N} \log F_n^{(t)}$, where $F_n^{(t)}$ is the average throughput of n^{th} UE over last t_c TTIs (between $(t-t_c)^{\text{th}}$ to $(t-1)^{\text{th}}$ TTI); $F_n^{(t)}$ for all UEs are updated before the next TTI, and the process repeats. $F_n^{(t)}$ can be calculated as follows:

$$F_n^{(t)} = \left(\frac{t_c - 1}{t_c}\right) F_n^{(t-1)} + \frac{1}{t_c} f_n^{(t-1)} \tag{8}$$

In addition, it can be proved that PF utility function of network (**U**) can be relaxed to the following non-logarithmic form [38]:

$$\mathbf{U} = \sum_{n=1}^{N} \frac{f_n^{(t)}}{F_n^{(t)}} = \sum_{n=1}^{N}\sum_{m=1}^{M}\sum_{p=1}^{P}\sum_{k=1}^{K} z^{k(t)}_{m,p,n} a^{k(t)}_{m,p,n} \tag{9}$$

where $z^{k(t)}_{m,p,n} = \frac{r^{k(t)}_{m,p,n}}{F_n^{(t)}}$.

To ensure fairness among UEs with different CA capabilities (μ_n), priority weight for each n^{th} UE is inversely proportional to its average throughput $F_n^{(t)}$, which is computed with respect to all RBs located over all CCs available in the cell. For simplicity, TTI notation for the rest of this article is omitted.

B. Optimisation problem

In this section, SCC selection, RB allocation and MCS assignment are formulated as a constrained joint optimisation problem with the objective of maximising the utility function **U**. The optimisation problem is defined as follows:

$$\max_{a,e} \quad \sum_{n=1}^{N}\sum_{m=1}^{M}\sum_{p=1}^{P}\sum_{k=1}^{K} z^k_{m,p,n} a^k_{m,p,n} \tag{10}$$

subject to:

$$\sum_{n=1}^{N}\sum_{k=1}^{K} a^k_{m,p,n} \leq 1 \tag{11}$$

$$\sum_{m=1}^{M}\sum_{k=1}^{K} e^k_{m,n} \leq \mu_n \tag{12}$$

$$a^k_{m,p,n} \leq e^k_{m,n} \tag{13}$$

$$\sum_{k=1}^{K} e^k_{m,n} \leq 1 \tag{14}$$

$$y_{m,n} \leq \sum_{k=1}^{K} e^k_{m,n} \tag{15}$$

$$e^k_{m,n}, a^k_{m,p,n} \in \{0,1\} \tag{16}$$

where $m \in \mathcal{M}, p \in \mathcal{P}, n \in \mathcal{N}$ and $k \in \mathcal{K}$. (11) ensures that each RB is assigned exclusively to maximum one UE. Furthermore, (12) satisfies CA restriction of each UE. (13) assures that p^{th} RB in m^{th} CC is allocated to n^{th} UE with k as a MCS-index value if and only if m^{th} CC is allocated to n^{th} UE with k; (14) guarantees that all allocated RBs to n^{th} UE in m^{th} CC have same MCS value. (15) is for that in case that m^{th} CC is selected as a PCC for n^{th} UE, one and only one $e^k_{m,n}$ should equal 1. Finally, constraint (16) assures that the optimisation problem is binary.

By solving the optimisation problem (10)-(16), RB allocations (across PCCs and SCCs), SCC allocations and MCS-index values can be obtained, and signalled to UEs.

V. Integer Linear Programming

A. Objective Function

The optimisation problem (10)-(16) belongs to an 0-1 ILP class of problems. The original optimisation problem does not have a canonical form, but can be converted to an equivalent problem by the transformation of variables, i.e. $a^k_{m,p,n}$, $z^k_{m,p,n}$ and $e^k_{m,n}$ can be ordered to construct vectors **a**, **z** and **e** respectively. The relationship between original variables and their corresponding vectors can be expressed as follows:

$$\mathbf{a} = \begin{bmatrix} \overline{a}_1 & \cdots & \overline{a}_i & \cdots & \overline{a}_{MPNK} \end{bmatrix}^T \tag{17}$$

$$\mathbf{z} = \begin{bmatrix} \overline{z}_1 & \cdots & \overline{z}_i & \cdots & \overline{z}_{MPNK} \end{bmatrix}^T \tag{18}$$

$$\mathbf{e} = \begin{bmatrix} \overline{e}_1 & \cdots & \overline{e}_j & \cdots & \overline{e}_{MNK} \end{bmatrix}^T \tag{19}$$

where $\overline{a}_i = a^k_{m,p,n}$, $\overline{z}_i = z^k_{m,p,n}$, $\overline{e}_j = e^k_{m,n}$ and

$$i = p + P(k-1) + PK(m-1) + PKM(n-1) \tag{20}$$

$$j = k + K(m-1) + KM(n-1) \tag{21}$$

The vectors **a** and **e** can be concatenated, and transposed into a new vector referred to as **x** with a dimension of $MPNK + MNK$ as follows:

$$\mathbf{x} = [\mathbf{a}^T, \mathbf{e}^T]^T \tag{22}$$

Similarly, constraint vector **g** with a dimension of $MPNK + MNK$ can be expressed as:

$$\mathbf{g} = [\mathbf{z}^T, \mathbf{0}^T_{MNK}]^T \tag{23}$$

Accordingly, objective function defined in (10) can be rewritten as:

$$\max_{\mathbf{x}} \ \mathbf{g}^T\mathbf{x} \tag{24}$$

B. Inequality Constraints

In this section, the constraints defined in (11)-(16) are converted into an equivalent canonical form. From (11):

$$C_1\mathbf{a} \preceq \mathbf{1} \tag{25}$$

where $C_1 = \begin{bmatrix} blkd(L_1, M) & \cdots & blkd(L_1, M) \end{bmatrix}_{MP \times MPNK}$ and $L_1 = \begin{bmatrix} I_P & \cdots & I_P \end{bmatrix}_{P \times PK}$. Similarly, (12) can be rewritten as:

$$C_2\mathbf{e} \preceq \boldsymbol{\mu} \tag{26}$$

where $\boldsymbol{\mu} = \begin{bmatrix} \mu_1 & \cdots & \mu_N \end{bmatrix}^T$ and $C_2 = blkd(\mathbf{1}_{MK}^T, N)$. Constraint (13) can be expressed as:

$$C_3\mathbf{x} \preceq \mathbf{0} \tag{27}$$

where $C_3 = \begin{bmatrix} I_{NKMP}, & L_3 \end{bmatrix}_{MPNK \times (MPNK+MNK)}$ and $L_3 = -blkd(\mathbf{1}_P, MNK)$. Similarly for (14):

$$C_4\mathbf{e} \preceq \mathbf{1} \tag{28}$$

where $C_4 = blkd(\mathbf{1}_K^T, MN)$. Finally, constraint (15) can be expressed as:

$$-C_4\mathbf{e} \preceq \mathbf{y} \tag{29}$$

where $\mathbf{y} = \begin{bmatrix} \overline{y}_1 & \cdots & \overline{y}_o & \cdots & \overline{y}_{MN} \end{bmatrix}^T$ with $\overline{y}_o = -y_{m,n}$ and suffix $o = m + M(n-1)$.
Accordingly, constraints (25)-(29), can be integrated as follows:

$$C\mathbf{x} \preceq \mathbf{q} \tag{30}$$

where C is the constraint matrix:

$$C = \begin{bmatrix} C_1^T & 0 & I_{MPNK} & 0 & 0 \\ 0 & C_2^T & L_3^T & C_4^T & -C_4^T \end{bmatrix}^T \tag{31}$$

and

$$\mathbf{q} = \begin{bmatrix} \mathbf{1}_{MP}^T & \boldsymbol{\mu}^T & \mathbf{0}_{MPNK}^T & \mathbf{1}_{MN}^T & \mathbf{y}^T \end{bmatrix}^T \tag{32}$$

Equivalently, the optimisation problem (10)-(16) can be rewritten as:

$$\max_{\mathbf{x}} \ \mathbf{g}^T\mathbf{x} \tag{33}$$

subject to:

$$\left\{ \mathbf{x} | C\mathbf{x} \preceq \mathbf{q}, \mathbf{x} \subseteq \mathbb{Z}^{(MPNK+MNK)} \right\} \tag{34}$$

Constraints (28) and (29) assure that the elements of $\mathbf{e}$ from polyhedron (34) contain only integer numbers 0s and 1s. However, constraint (27) implies that the elements of $\mathbf{a}$ from polyhedron (34) has any integer number with maximum of 1. Furthermore, we will show in next section that the optimum values of $\mathbf{a}$ (or $\mathbf{x}$) are binary (0s and 1s) regardless that the polyhedron (34) contains negative integers of $\mathbf{a}$.

C. Linear Programming Relaxation

As mentioned in Section V-A, the optimisation problem (10)-(16), or its equivalent (33)-(34), belongs to 0-1 ILPs. There are variety of algorithms that can be used to solve ILPs, however, no polynomial-time algorithm has been discovered. One obvious solution is enumeration - systematically checking all feasible solutions, and finding one with the maximum objective value - which is difficult, time-consuming and practically unsolvable, especially for the large-scale ILPs such as (33)-(34). In fact, the ILPs are regarded as NP-complete (when the problem is both in NP and NP-hard) [39], [40]. However, such problems can be solved efficiently under certain conditions such as total unimodularity and total dual integrality [39].

The solution set of a finite number of inequalities can be defined as a polyhedron [41]:

$$\Theta = \{\mathbf{x} | C\mathbf{x} \preceq \mathbf{q}\} \tag{35}$$

where Θ is convex, and there always is an optimum solution which is one of the finitely many extreme points.

Definition 1 (Integral Polyhedron): A polyhedron Θ is called integral if every nonempty face of Θ contains an integral point, i.e. if Θ is the convex hull of the integral vectors contained in it [39].

Total unimodularity and total dual integrality are sufficient conditions in which Θ is integral, in other words if C and $\mathbf{q}$ satisfy certain properties then Θ can be concluded as an integral. Total unimodularity can be applied for any arbitrary integral $\mathbf{q}$, but total dual integrality requires only specific class of integral $\mathbf{q}$ - total dual integrality is a weaker sufficient condition for integrality than total unimodularity. In this article, total unimodularity is used to prove that Θ is integral for any arbitrary integral vector $\mathbf{q}$ (which is dependent on CA capabilities of UEs).

Definition 2 (Total Unimodular Matrix): A matrix C is total unimodular if determinant of its every square sub-matrix equals $-1, 0, 1$ [39].

Theorem 1 (Hoffman and Kruskal's Theorem): Let C be an integral matrix, then C is totally unimodular if and only if for each integral vector $\mathbf{q}$ the polyhedron $\{\mathbf{x} | C\mathbf{x} \preceq \mathbf{q}, \mathbf{0} \preceq \mathbf{x}\}$ is integral [42], [43].

Lemma 1: The constraint matrix C defined in (31) is TUM (the proof is given in the Appendix).

Since C is TUM, according to **Theorem 1**, $\{\mathbf{x} | C\mathbf{x} \preceq \mathbf{q}, \mathbf{0} \preceq \mathbf{x}\}$ is integral. Moreover, constraints (27), (28) and (29) - which are already included in $C\mathbf{x} \preceq \mathbf{q}$ - make the following set of equalities:

$$\{\mathbf{x} | C\mathbf{x} \preceq \mathbf{q}, \mathbf{0} \preceq \mathbf{x}\} = \{\mathbf{x} | C\mathbf{x} \preceq \mathbf{q}, \mathbf{0} \preceq \mathbf{x} \preceq \mathbf{1}\} \tag{36}$$

Thus, we can conclude that integral polyhedron $\{\mathbf{x} | C\mathbf{x} \preceq \mathbf{q}, \mathbf{0} \preceq \mathbf{x}\}$ contains only 0s and 1s (implying the negative integers will not be in the optimum solution - as mentioned in previous section) which satisfies the binary constraint (16). A link between integral polyhedron and LP is given by the following theorem:

Theorem 2: Consider an LP of the form:

$$\max_{\mathbf{x}} \ \mathbf{g}^T\mathbf{x} \tag{37}$$

$$\{\mathbf{x}|C\mathbf{x} \preceq \mathbf{q}, \mathbf{0} \preceq \mathbf{x}\} \tag{38}$$

if the problem's polyhedron $\{\mathbf{x}|C\mathbf{x} \preceq \mathbf{q}, \mathbf{0} \preceq \mathbf{x}\}$ is integral, then the LP has an integral optimal solution (its proof is given in [44]).

According to **Theorem 2**, the 0-1 ILP defined in (33)-(34) can be relaxed to the LP mentioned in (37)-(38), and then can be solved (the optimal basic solution is guaranteed to be binary). Schematically, a visual diagram of the concepts taken for LP relaxation is shown in Fig. 1.

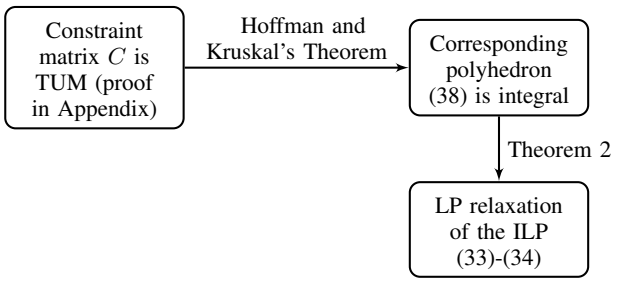

Fig. 1: The schematic proof of the LP relaxation

VI. Computational Complexity Analysis

There is no simple analytical formula for solution of LPs, but there are a variety of very effective methods for solving them, including Dantzig's simplex algorithm [45], interior point method [46] and Ellipsoid method [47]. In contrast to interior point and Ellipsoid methods, no variant of the simplex algorithm is polynomial-time algorithm (in the worst-case scenario, it may require a very large number of steps which depends exponentially on the problem dimension), but in practice it has proved to be a very efficient and reliable method. The Ellipsoid method - the first polynomial-time algorithm for LPs - is too inefficient to be used in practice, because the per-iteration cost of the linear algebra operations to update the ellipsoids is too high [42].

Interior point methods low degree polynomial worst-case complexity, and an almost constant number of iterations which depends very little, if at all, on the problem dimension, make them particularly attractive for very large scale optimisation [48]. Interior point methods are competitive when dealing with small problems of dimensions, and are beyond competition when applied to large problems of dimensions going into millions of constraints and variables [49].

The LP (37)-(38) is of order $(N + MP) \times (MPNK + MNK)$ maximising $\mathbf{g}^T\mathbf{x}$ over all $\mathbf{x}$ in $\mathbb{R}^{(MPNK+MNK)}$ such that $C\mathbf{x} \preceq \mathbf{q}$. In this work, since the mentioned problem's dimension is high, a family of interior point method named primal Newton barrier method [50] is employed. Barrier methods for LPs generate approximations to both the primal and dual variables at each iteration. The formulation of the barrier requires the specification of a bounded sequence ϵ that determines the accuracy of the solutions of the problem. In this work, we assume that $\epsilon = 10^{-4}$.

It is not possible to give the exact number of arithmetic operations required to solve LPs [41], however, Robere *et al.* [50] established higher bound on the number of operations required to solve LPs, to a given accuracy ϵ, using primal Newton barrier method. According to [50], the worst-case complexity of solving the optimisation problem of (37) and (38) equals $\mathcal{O}(\sqrt{N + MP + MPNK + MNK}\ln\frac{1}{\epsilon})$. Since P, K and M are relatively small numbers, the worst-case scenario is investigated as the number of UEs approaches infinity:

$$\lim_{N\to\infty} \mathcal{O}(\sqrt{N + MP + NMPK + NMK}\ln\frac{1}{\epsilon}) \approx \mathcal{O}(\delta N^{(\frac{1}{2})}) \tag{39}$$

where δ is a constant number. Liao *et al.* [25] obtained the computational complexity of GA as $\mathcal{O}(NPK(M + N\max(\mu_n) - 1))$. Similarly, for large N, GA's complexity approaches to:

$$\lim_{N\to\infty} \mathcal{O}(NPK(M + N\max(\mu_n) - 1)) \approx \mathcal{O}(\delta^* N^2) \tag{40}$$

where δ^* is a constant number. As it can be seen from (39) and (40), computational complexity of ORAA is much less than GA.

VII. Simulation Results and Discussion

In this section, a set of system-level performance results are presented in order to compare, and show the efficiency of ORAA over GA [25]. Network-centric KPIs such as overall network throughput and CC spectral efficiency are demonstrated. Moreover QoS at UE level, measured by UE throughput and throughput fairness to the benefit of UEs are shown. The simulation results demonstrate high potential of the proposed method in terms of both system and user-level efficiency.

A. Network Geometry and Channel Model Parameters

To investigate network performance, dynamic simulations are performed, and UEs are distributed independently under three UE deployment scenarios, 1) random, 2) cell center, and 3) cell edge. In random deployment, UEs are distributed with uniform distribution within each cell whereas in cell center and cell edge, UEs are distributed near the cell center and cell edge, respectively. The cellular environment is consisted of 7 microcells, and each has 10 UEs. A site layout of 7 cells wrap-around is employed to obtain the numerical results.

The simulation results are performed in an urban area where the cell radius is 500 m, and the base station antenna height is 15 m above average rooftop level; antennas of 3 dB beam width of $\theta_{3dB} = 65°$, and maximum attenuation of $A_m = 15$ dBi is used in each cell.

Furthermore, DL performance is assessed in two different CA scenarios: Single frequency Band (SB) and Multi frequency Band (MB). In SB scenario, it is assumed that each CC is of 5 MHz, and each cell has been configured for 6 CCs all located in 2 GHz band. In MB scenario, simulations are conducted for 3 CCs in 2 GHz (Higher Band - HB), and 3 CCs in 900 MHz (Lower Band - LB).

Each of the channels for LB and HB are modeled as flat Rayleigh channel with penetration loss of 20 dB, and path loss model of $P_{LB} = 120.9 + 37.6\log_{10} R$ (R is distance in km) and $P_{HB} = 128.1 + 37.6\log_{10} R$ respectively. The mean

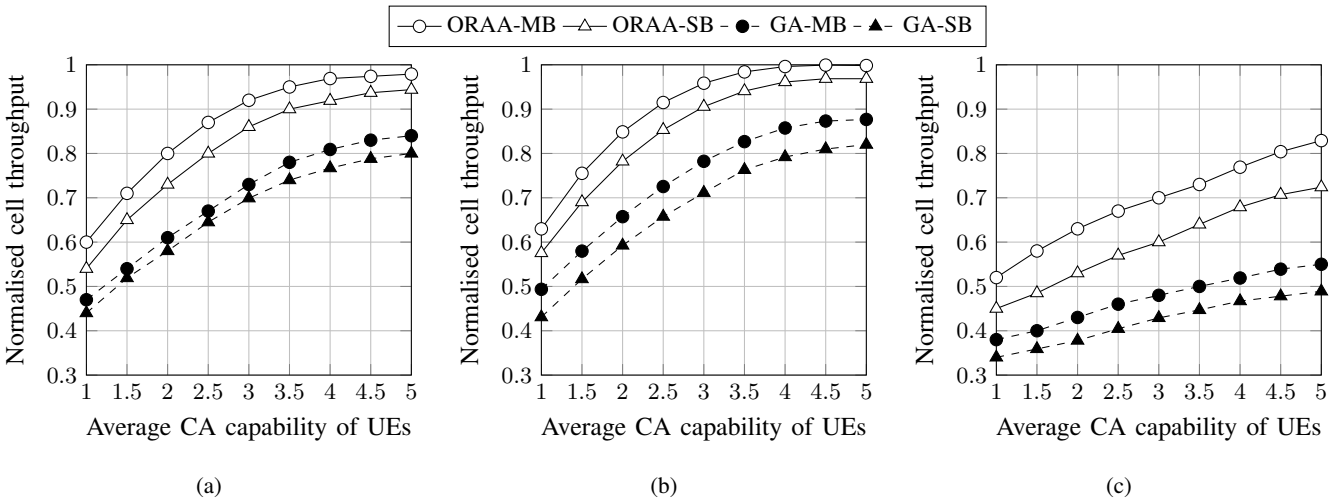

Fig. 2: The impact of CA capability and multi-band accessibility of UEs on cell throughput when $\overline{\mu}$ increases in the network, and $N = 10$, (a) random deployment (b) cell-center deployment (c) cell-edge deployment

and standard deviation of log-normal fading are 0 and 8 dB respectively. The multipath intensity profile of the Pedestrian-A channel - which requires users with low mobility ($\leq$ 3 km/h) - is considered.

MATLAB-based standard compliant system-level simulator [14] has been utilised to simulate the network scenarios, and evaluate performance of the proposed algorithm. The number of UEs per cell (including LTE and LTE-A) is 10, and all UEs are moving at a walking speed of 3 km/h. Each simulation scenario lasts for $10,000$ TTIs or 10 seconds, and repeated 100 times for averaging results. Other simulation parameters are summarised in TABLE II.

TABLE II: Simulation parameters

Parameter	Value
M	6
N	10
P	25
t_c	100
Cyclic-prefix length	4.7 μs
Total transmit power	46 dBm (40 W)
Inter-cell distance	1 km
Site layout	7 Cells wrap-around
Traffic model	Backlogged

B. Throughput of a Cell

Fig. 2 shows average normalised values of cell throughput as a function of average CA capability of UEs in the cell, defined as $\overline{\mu} = \sum_{n=1}^{N} \mu_n$, where $\overline{\mu} = 1$ represents the case when all UEs are LTE Rel-8 terminals, and $\overline{\mu} = 5$ represents the case when all UEs are LTE-A Rel-10 devices, and can aggregate up to 5 CCs. As seen from Fig. 2, regardless of network deployment, UEs in the cell with higher $\overline{\mu}$ have higher probability to utilise higher-rate RBs available in the network. Therefore, for both algorithms (i.e. GA and ORAA) in both scenarios (SB and MB), and all three deployment scenarios cell throughput increases with CA capability of UEs. This can be explained by the fact that in case of higher CA capability, UEs can utilise higher bandwidth and higher frequency diversity. Furthermore, since the achievable throughput of UEs is limited by the available SNR to UEs (especially cell-edge UEs), increasing transmission bandwidth provides high data rates to cell-edge UEs, and eventually increases cell throughput.

Additionally, Fig. 2 confirms the preliminary simulation results on CA [51] which evaluates DL performance gain of CA, relative to the simple approach of deploying multiple independent CCs on eNB. [51] shows that at the same light or medium traffic load, the mean throughput of CA-based systems is approximately twice that of non-CA based systems. However, in case of this article, because of using backlogged traffic model, performance of CA-enabled scenario ($\overline{\mu} = 5$) is slightly less than twice of non-aggregating case ($\overline{\mu} = 1$).

Moreover, in MB scenario, because UEs are allowed to operate on lower frequency band, cell-edge UEs experience better channel quality than SB, leading to improved cell throughput of both ORAA and GA. As can be seen in Fig. 2 (a) and Fig. 2 (b), because of the limited number of CCs in the cell (only 6), and better SNR conditions in random and cell-center deployments for $\overline{\mu} \geq 4$, cell throughput does not improve further, however in case of cell-edge deployment (Fig. 2 (c)), cell throughput still increases. Interestingly, there is a sharp increase in cell throughput from $\overline{\mu} = 1$ to 1.5, and the reason is that if $\overline{\mu} = 1$, the only CC (precisely PCC) is selected based on RSRP level. However if $\overline{\mu} > 1$, SCCs are selected by RRM entity based on CQI reports. The cell throughput of ORAA significantly outperforms GA in both SB and MB scenarios in all three different deployments.

Fig. 3 shows a comparison of cell throughput as a function of number of UEs in both scenarios (SB, MB), and all three deployment scenarios when $\overline{\mu} = 3$. Similar to the case of increasing $\overline{\mu}$, increasing N improves cell throughput in all cases. When N increases in the cell, it enhances the likelihood that available RBs are assigned to UEs with better channel quality. Hence, by exploiting multiuser diversity, cell throughput improves in all cases. However, when there are

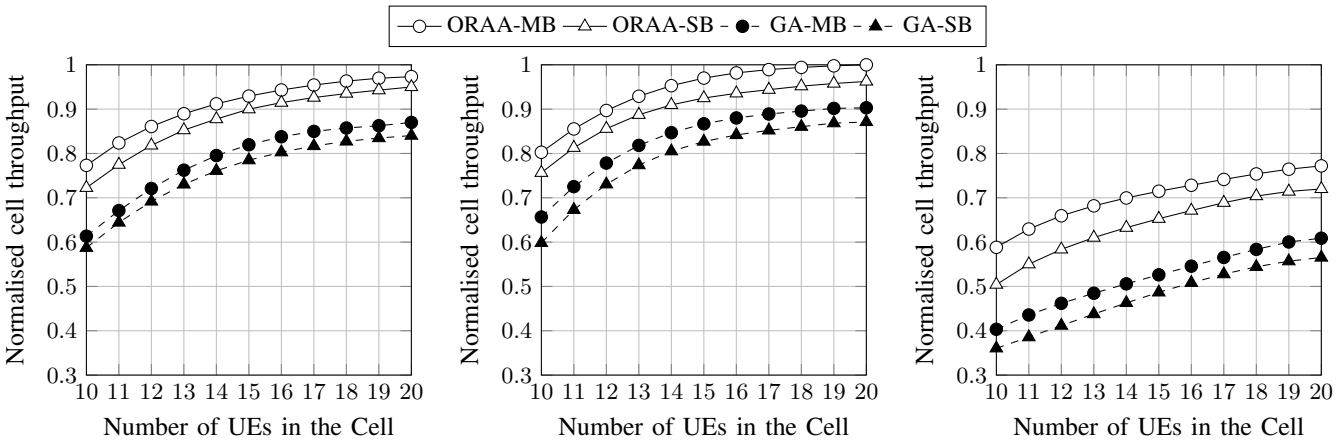

Fig. 3: The impact of CA capability and multi-band accessibility of UEs on cell throughput when N increases in the network, and $\overline{\mu} = 3$, (a) random deployment (b) cell-center deployment (c) cell-edge deployment

too many UEs in the cell, all available RBs in the cell are shared exclusively between them, and therefore fewer RBs are assigned to UEs. Therefore, cell throughout of all cases improves slightly as the number of UEs increases. Cell throughput of ORAA outperforms GA in both SB and MB scenarios, and in all deployment scenarios.

C. Throughput of UEs

Normalised throughput of individual UEs in three different deployment scenarios when $N = 10$ is shown in Fig. 4. UE label is ordered based on CA capabilities of UEs, i.e. the label is formatted as $n(\mu_n)$. For instance, in case of $1(1)$ and $2(1)$, 1^{st} and 2^{ed} UEs can utilise only one CC, but $9(5)$ and $10(5)$ mean 9^{th} and 10^{th} UE can aggregate up to five different CCs. As shown in Fig. 4, most of time, ORAA in MB scenario provides highest throughput to each UE. UEs with higher CA capability have slightly better throughput than others. If the priority weight of each user is computed with respect to all RBs located over its corresponding CC, the gap between throughput of UEs with one and two CCs aggregation capability, i.e. $1(1)$, $2(1)$ and $3(2)$, $4(2)$, could be bigger, and could lead to unfair RB distribution for non LTE-A UEs. But as mentioned in Section IV, we consider priority weight of n^{th} UE as an inversely proportional to its average throughput F_n which is computed with respect to all RBs located over all CCs available in the cell. As expected, in cell-centre deployment scenario (Fig. 4 (b)), UEs experience better throughput than random deployment (Fig. 4 (a)) and cell-edge deployment (Fig. 4 (c)).

In Fig. 5, throughput distribution of UEs in random deployment scenario is considered; UE label is ordered based on their overall average RSRP level, 1^{st} UE has the highest RSRP, and 10^{th} UE has the lowest average RSRP. For simplicity and comparison purposes, we assume that all UEs can aggregate same number of CCs, i.e. 4. In both ORAA and GA, throughput of UEs reduces by decreasing RSRP level, however in case of ORAA, cell-edge UEs experience better throughput than GA. ORAA assigns CC efficiently in such a way that RBs belong to HB CCs are mostly allocated to cell-center UEs and RBs from LB CCs are allocated to cell-edge UEs.

Similarly, in Fig. 6, Cumulative Distribution Function (CDF) of UEs throughput in the random deployment scenario is shown, throughput of UEs is averaged, and the CDF curves of the averaged throughput for four cases are shown. In case of ORAA-MB, 55% of UEs, as for GA-MB, 90% of UEs have throughput less than 0.6. From Fig. 5 and Fig. 6, it can be concluded that cell-edge UEs throughput can be improved by ORAA, while throughput of cell-center UEs remains similar to GA.

D. Throughput Fairness

In order to compare throughput fairness among UEs in the cell, Jain's fairness index [52] can be applied as follows:

$$T = \frac{(\sum_{n=1}^{N} f_n)^2}{N \sum_{n=1}^{N} f_n^2} \tag{41}$$

The value of T ranges from $\frac{1}{N}$ to 1, and $T = 1$ indicates that all UEs have equal throughput in average. Fig. 7 depicts the fairness index for different number of UEs, and it can be seen the fairness index is almost same for both ORAA and GA. ORAA outperforms slightly better than GA for smaller N, partially because of providing higher throughput for cell-edge UEs. However, for bigger N, GA presents fairer allocation than ORAA.

E. Component Carrier Spectral Efficiency

In this section, spectral efficiency (bits/s/Hz) per CC, representing overall throughput per bandwidth unit in each CC is investigated. CC spectral efficiency can be interpreted for load balancing which may avoid situations in which multiple UEs compete for RBs in a single CC while RBs in other CCs are wasted. For optimal system performance, it is desirable to have approximately equal load on different CCs. As seen in

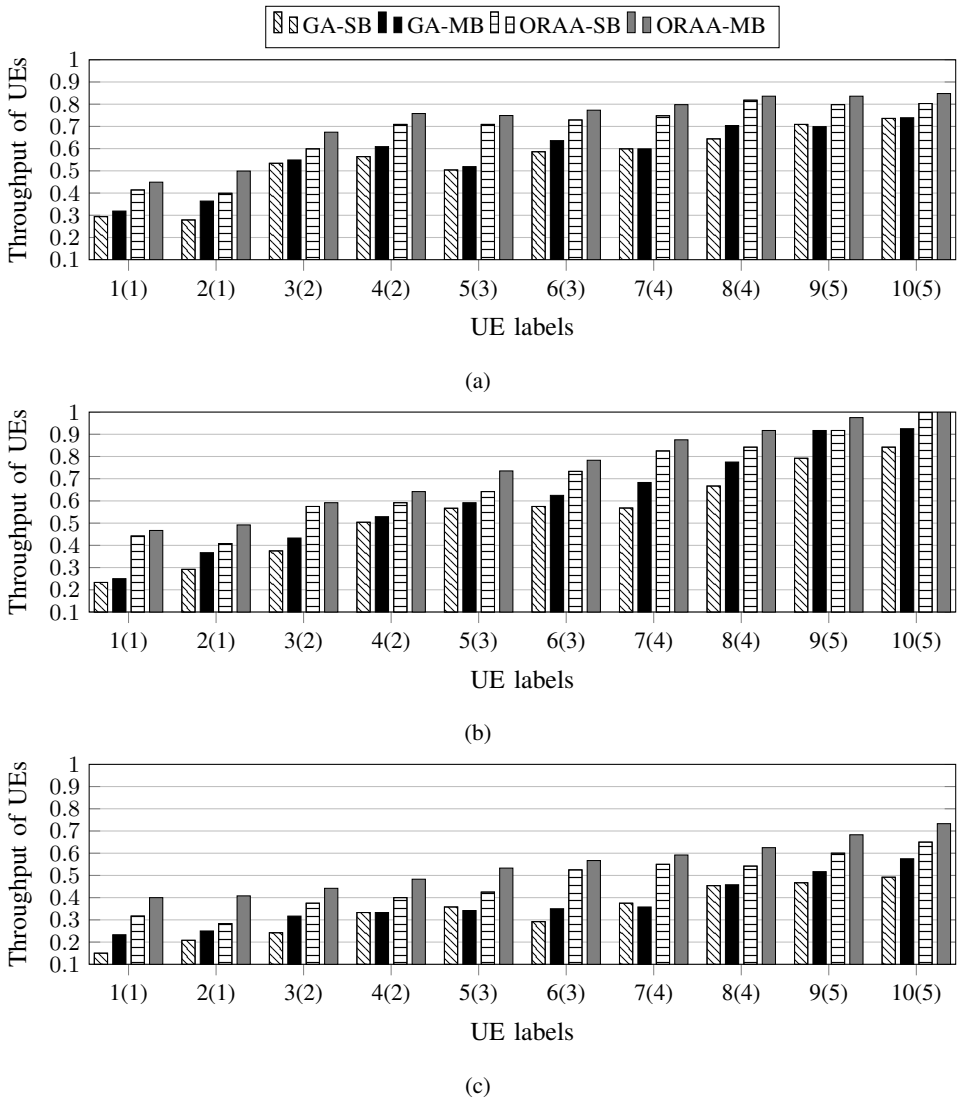

Fig. 4: The impact of CA capability and multi-band accessibility of UEs on normalised throughput of each UE ($N = 10$, $\overline{\mu} = 3$), (a) random deployment (b) cell-center deployment (c) cell-edge deployment

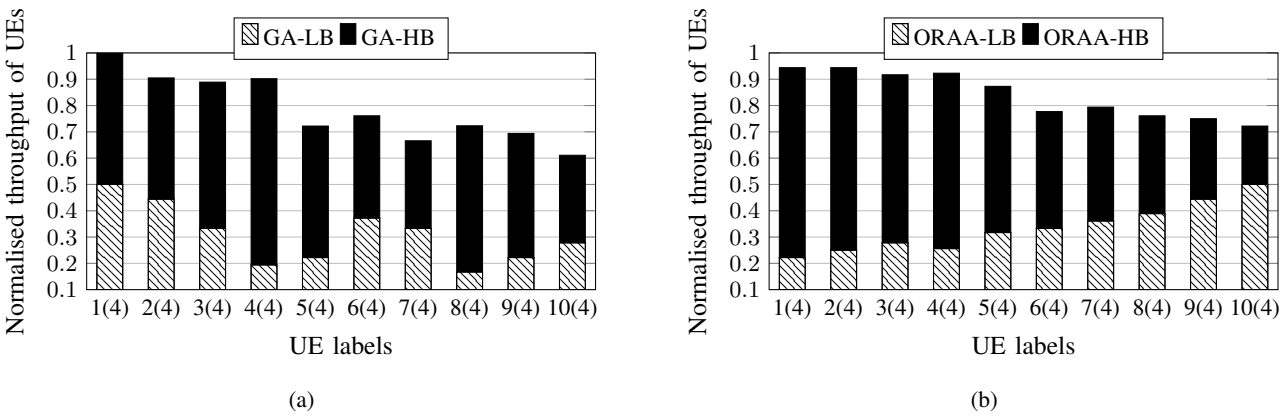

Fig. 5: Throughput distribution of UEs operating in MB spectrum in random deployment scenario ($N = 10$, $\overline{\mu} = 4$)

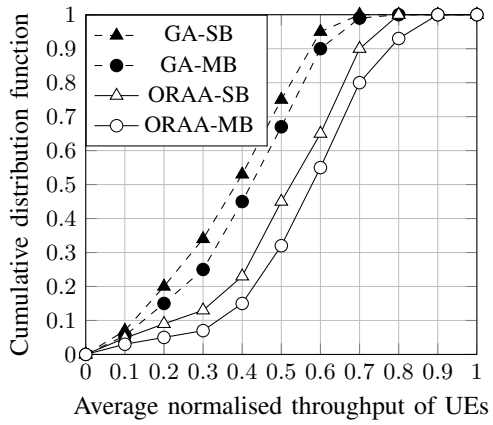

Fig. 6: CDF of UEs throughput in the cell for random deployment scenario ($N = 10$, $\overline{\mu} = 3$)

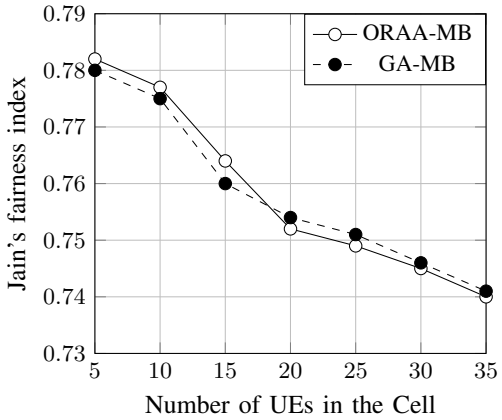

Fig. 7: Fairness index (41) as function of N from 5 to 35 ($\overline{\mu} = 3$)

Fig. 8, introducing LB CCs increases spectral efficiency even in HB CCs because of allocating LB CCs to cell-edge UEs. As it is expected, ORAA provides better CC spectral efficiency than GA, and distributes load in such a way that prevents from overloaded CC in the cell; maintaining appropriate UE experience and system performance.

F. Solution Analysis

The objective of ORAA is to allocate RBs to UEs optimally from multiple CCs; in addition, every UE subscribing for the mobile service is guaranteed to have a fair share of RBs while maximising cell throughput. For each UE, ORAA selects one or multiple CCs that provides maximum contribution to cell throughput.

Interestingly, as it is proven CA-enabled RRM in LTE-A networks with flat energy distribution over all RBs can be solved optimally using LP techniques instead of combinatorial or greedy algorithms. Duality gap, difference between the optimal primal and relaxed problem, is zero, and the computationally-efficient solution offered above coincides with the optimal solution. Complexity of ORAA is almost negligible compared with the complexity of GA.

VIII. Conclusions

In this article, RRM function of LTE-A with CA is formulated as the ILP, considering standard-compliant LTE constraints, such as MCS and CA constraints. We proved that the given ILP can be relaxed to the LP, and can be solved by means of LP techniques optimally. An optimum-efficient LTE-compliant solution based on PF scheduling is proposed. The simulation results demonstrate the high potential of proposed method, in terms of efficiency on the system and UE-levels. The results show that ORAA offers significant gains in overall network throughput and CC spectral efficiency to the benefit of MNOs. Moreover, the results show improvement in QoS of UEs, measured by UE throughput especially cell-edge UEs. For future work, we plan to consider RRM with considering inter-cell interference coordination with MIMO techniques which are other main features of LTE-A.

Appendix
Proof: Constraint Matrix C is Totally Unimodular

If a matrix T is TUM, then a matrix $T^{'}$ obtained from T by any one of the following operations is still TUM, i.e. TUM is preserved under the following operations:

Rule1: Multiplying a row or column by -1 [39], [53];

Rule2: Performing pivoting on any non-zero entry of a matrix [54];

Rule3: Deleting repeated rows or columns [39], [53], or duplicating rows or columns;

Rule4: Deleting or adding rows or columns containing only 0s except one non-zero element equals 1 [39], [53];

In this work, backward proof procedure is applied to prove that C is TUM. Initially, it is assumed that C (31) is TUM:

Step1: Multiplying a set of rows ($\begin{bmatrix}0 & -C_4\end{bmatrix}$) of C with -1 - Rule1:

$$C^{(1)} = \begin{bmatrix} C_1^T & 0 & I_{MNPK} & 0 & \boldsymbol{0} \\ 0 & C_2^T & L_3^T & C_4^T & \boldsymbol{C_4^T} \end{bmatrix}^T \tag{42}$$

Step2: Removing a set of repeated rows ($\begin{bmatrix}0 & C_4\end{bmatrix}$) of $C^{(1)}$ - Rule3:

$$C^{(2)} = \begin{bmatrix} C_1^T & 0 & I_{MNPK} & 0 \\ 0 & C_2^T & L_3^T & C_4^T \end{bmatrix}^T \tag{43}$$

Step3: Pivoting over all 1's elements of I_{MNPK} - Rule2:

$$C^{(3)} = \begin{bmatrix} \boldsymbol{0} & 0 & I_{MNPK} & 0 \\ \boldsymbol{D^T} & C_2^T & L_3^T & C_4^T \end{bmatrix}^T \tag{44}$$

where $D = \begin{bmatrix} blkd(1_{P\times K}, M) & \cdots & blkd(1_{P\times K}, M) \end{bmatrix}_{MP\times MNK}$

Step4: Because a set of columns ($\begin{bmatrix}0 & 0 & I_{MNPK} & 0\end{bmatrix}^T$) of $C^{(3)}$ contain only one non-zero element in each column, $\begin{bmatrix}0 & 0 & I_{MNPK} & 0\end{bmatrix}^T$ can be removed - Rule4:

$$C^{(4)} = \begin{bmatrix} D^T & C_2^T & L_3^T & C_4^T \end{bmatrix}^T \tag{45}$$

Step5: Each row of L_3 is repeated P times; therefore according to Rule3, the repeated rows can be removed, and L_3 can be converted to $-I_{NKM}$. Therefore, $C^{(5)}$ can be obtained as follows:

$$C^{(5)} = \begin{bmatrix} D^T & C_2^T & \boldsymbol{-I_{MNK}} & C_4^T \end{bmatrix}^T \tag{46}$$

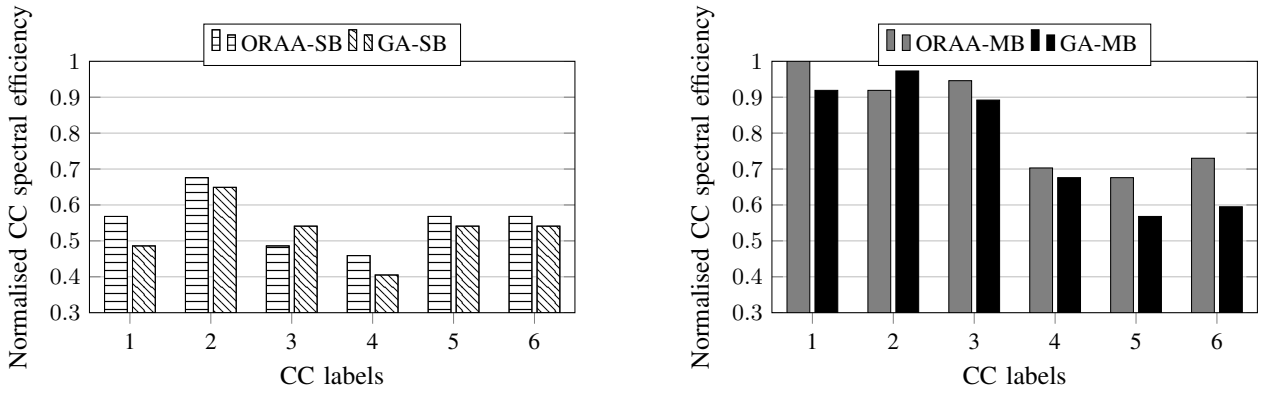

(a) (b)

Fig. 8: CC spectral efficiency ($N = 10$, $\overline{\mu} = 3$), (a) all CCs $\{1, 2, 3, 4, 5, 6\}$ are based on 2 GHz band, (b) CCs $\{1, 2, 3\}$ are located in 900 MHz band, but CCs $\{4, 5, 6\}$ belong to 2 GHz band.

Step6: Multiplying a set of rows $(-I_{MNK})$ of $C^{(5)}$ with -1 - Rule1:

$$C^{(6)} = \begin{bmatrix} D^T & C_2^T & \boldsymbol{I_{MNK}} & C_4^T \end{bmatrix}^T \tag{47}$$

Step7: Pivoting over all 1's elements of I_{MNK} - Rule2:

$$C^{(7)} = \begin{bmatrix} \mathbf{0} & \mathbf{0} & I_{MNK} & \mathbf{0} \end{bmatrix}^T \tag{48}$$

Step8: Removing a set of all-zero rows:

$$C^{(8)} = I_{MNK} \tag{49}$$

where I_{MNK} is TUM. All of the mentioned steps also preserve unimodularity in backward (from Step8 to Step1). Therefore, it can be concluded that C is TUM.

REFERENCES

[1] C. Wijting *et al.*, "Key Technologies for IMT-Advanced Mobile Communication Systems," *Wireless Communications, IEEE*, vol. 16, no. 3, pp. 76–85, June 2009.

[2] "Background on IMT-Advanced," ITU-R, Tech. Rep., IMT-ADV/1-E, May. 2008.

[3] "Further Advancements for E-UTRA Physical Layer Aspects,," 3GPP Technical Report 36.814, Tech. Rep., Mar. 2010. [Online]. Available: http://www.3gpp.org.

[4] "Feasibility study for Further Advancements for E-UTRA (LTE-Advanced),," 3GPP Technical Report 36.912, Tech. Rep., Mar. 2010. [Online]. Available: http://www.3gpp.org.

[5] P. Mogensen *et al.*, "Lte-advanced: The path towards gigabit/s in wireless mobile communications," in *Wireless Communication, Vehicular Technology, Information Theory and Aerospace Electronic Systems Technology, 2009. Wireless VITAE 2009. 1st International Conference on*, May 2009, pp. 147–151.

[6] S. Parkvall, E. Dahlman, A. Furuskar, Y. Jading, M. Olsson, S. Wanstedt, and K. Zangi, "Lte-advanced - evolving lte towards imt-advanced," in *Vehicular Technology Conference, 2008. VTC 2008-Fall. IEEE 68th*, Sept 2008, pp. 1–5.

[7] B. M. B. K.R. Rao, Zoran S. Bojkovic, *Wireless Multimedia Communication Systems: Design, Analysis, and Implementation,*. CRC Press, 2014.

[8] "Dl carrier aggregation performance in heterogeneous networks," 3GPP TSG RAN WG1 #58, R1-093145, Tech. Rep.

[9] S. Rostami, K. Arshad, and P. Rapajic, "Aggregation-based spectrum assignment in cognitive radio networks," in *Advanced Computing and Communication Systems (ICACCS), 2013 International Conference on*, Dec 2013, pp. 1–6.

[10] H. Lee, S. Vahid, and K. Moessner, "A survey of radio resource management for spectrum aggregation in lte-advanced," *Communications Surveys Tutorials, IEEE*, vol. 16, no. 2, pp. 745–760, Second 2014.

[11] M. Sternad, T. Svensson, T. Ottosson, A. Ahlen, A. Svensson, and A. Brunstrom, "Towards systems beyond 3g based on adaptive ofdma transmission," *Proceedings of the IEEE*, vol. 95, no. 12, pp. 2432–2455, Dec 2007.

[12] K. Pedersen, T. Kolding, F. Frederiksen, I. Kovacs, D. Laselva, and P. Mogensen, "An overview of downlink radio resource management for utran long-term evolution," *Communications Magazine, IEEE*, vol. 47, no. 7, pp. 86–93, July 2009.

[13] J. Zyren, "White paper overview of the 3gpp long term evolution physical layer," July 2007.

[14] J. Ikuno, M. Wrulich, and M. Rupp, "System level simulation of lte networks," in *Vehicular Technology Conference (VTC 2010-Spring), 2010 IEEE 71st*, May 2010, pp. 1–5.

[15] "Lte; evolved universal terrestrial radio access (e-utra);physical layer procedures,," 3GPP TS 36.213 version 10.1.0 Release 10, Tech. Rep., APR. 2010. [Online]. Available: http://www.3gpp.org.

[16] G. Yuan, X. Zhang, W. Wang, and Y. Yang, "Carrier aggregation for lte-advanced mobile communication systems," *Communications Magazine, IEEE*, vol. 48, no. 2, pp. 88–93, February 2010.

[17] L. Garcia, K. Pedersen, and P. Mogensen, "Autonomous component carrier selection: interference management in local area environments for lte-advanced," *Communications Magazine, IEEE*, vol. 47, no. 9, pp. 110–116, September 2009.

[18] J. Xiao, R. Hu, Y. Qian, L. Gong, and B. Wang, "Expanding lte network spectrum with cognitive radios: From concept to implementation," *Wireless Communications, IEEE*, vol. 20, no. 2, pp. 12–19, April 2013.

[19] S. P. Erik Dahlman and J. Skld, *4G LTE/LTE-Advanced for Mobile Broadband*. Academic Press, 2011.

[20] K. Sundaresan and S. Rangarajan, "Energy efficient carrier aggregation algorithms for next generation cellular networks," in *Network Protocols (ICNP), 2013 21st IEEE International Conference on*, Oct 2013, pp. 1–10.

[21] L. Giupponi, R. Agusti, J. Perez-Romero, and O. Sallent, "Inter-operator agreements based on qos metrics for improved revenue and spectrum efficiency," *Electronics Letters*, vol. 44, no. 4, pp. 303–304, February 2008.

[22] H. Wang, C. Rosa, and K. Pedersen, "Uplink component carrier selection for lte-advanced systems with carrier aggregation," in *Communications (ICC), 2011 IEEE International Conference on*, June 2011, pp. 1–5.

[23] F. Capozzi, G. Piro, L. Grieco, G. Boggia, and P. Camarda, "Downlink packet scheduling in lte cellular networks: Key design issues and a survey," *Communications Surveys Tutorials, IEEE*, vol. 15, no. 2, pp. 678–700, Second 2013.

[24] S. Ahmadi, *A Practical Systems Approach to Understanding 3GPP LTE Releases 10 and 11 Radio Access Technologies*. Academic Press, 2014.

[25] H.-S. Liao, P.-Y. Chen, and W.-T. Chen, "An efficient downlink radio resource allocation with carrier aggregation in lte-advanced networks,"

Mobile Computing, IEEE Transactions on, vol. PP, no. 99, pp. 1–1, 2014.

[26] S. Rostami, K. Arshad, and P. Rapajic, "A joint resource allocation and link adaptation algorithm with carrier aggregation for 5g lte-advanced network," in *Telecommunications (ICT), 2015 22ed International Conference on*, April 2015.

[27] H. Tian, S. Gao, J. Zhu, and L. Chen, "Improved Component Carrier Selection Method for Non-Continuous Carrier Aggregation in LTE-Advanced Systems," in *Vehicular Technology Conference (VTC Fall), 2011 IEEE*, Sept 2011, pp. 1–5.

[28] F. Wu, Y. Mao, S. Leng, and X. Huang, "A carrier aggregation based resource allocation scheme for pervasive wireless networks," in *Dependable, Autonomic and Secure Computing (DASC), 2011 IEEE Ninth International Conference on*, Dec 2011, pp. 196–201.

[29] Z. Huang, Y. Ji, and B. Zhao, "An efficient resource allocation algorithm with carrier aggregation in lte advanced systems," in *Wireless Communications Signal Processing (WCSP), 2012 International Conference on*, Oct 2012, pp. 1–6.

[30] X. Cheng, G. Gupta, and P. Mohapatra, "Joint carrier aggregation and packet scheduling in lte-advanced networks," in *Sensor, Mesh and Ad Hoc Communications and Networks (SECON), 2013 10th Annual IEEE Communications Society Conference on*, June 2013, pp. 469–477.

[31] J. Niu, T. Su, G. Li, D. Lee, and Y. Fu, "Joint transmission mode selection and scheduling in lte downlink mimo systems," *Wireless Communications Letters, IEEE*, vol. 3, no. 2, pp. 173–176, April 2014.

[32] J. Huang, V. Subramanian, R. Agrawal, and R. Berry, "Downlink scheduling and resource allocation for ofdm systems," *Wireless Communications, IEEE Transactions on*, vol. 8, no. 1, pp. 288–296, Jan 2009.

[33] W. Ho and Y.-C. Liang, "Optimal resource allocation for multiuser mimo-ofdm systems with user rate constraints," *Vehicular Technology, IEEE Transactions on*, vol. 58, no. 3, pp. 1190–1203, March 2009.

[34] S. Rostami, K. Arshad, and P. Rapajic, "Resource allocation algorithms for OFDM based wireless systems," in *2015 IEEE 26th Annual International Symposium on Personal, Indoor and Mobile Radio Communications - (PIMRC)*, Hong Kong, P.R. China, Aug. 2015, pp. 1268–1273.

[35] L. Hoo, B. Halder, J. Tellado, and J. Cioffi, "Multiuser transmit optimization for multicarrier broadcast channels: asymptotic fdma capacity region and algorithms," *Communications, IEEE Transactions on*, vol. 52, no. 6, pp. 922–930, June 2004.

[36] W. Yu and J. Cioffi, "Constant-power waterfilling: performance bound and low-complexity implementation," *Communications, IEEE Transactions on*, vol. 54, no. 1, pp. 23–28, Jan 2006.

[37] Y. Wang, K. Pedersen, T. Sorensen, and P. Mogensen, "Carrier load balancing and packet scheduling for multi-carrier systems," *Wireless Communications, IEEE Transactions on*, vol. 9, no. 5, pp. 1780–1789, May 2010.

[38] H. J. Kushner and P. A. Whiting, "Asymptotic properties of proportional-fair sharing algorithms," DTIC Document, Tech. Rep., 2002.

[39] A. Schrijver, *Theory of Linear and Integer Programming*. John Wiley & Sons, Chichester, 1986.

[40] E. T. Hubertus Th. Jongen, Klaus Meer, *Optimization Theory*. Springer, 2004.

[41] S. Boyd and L. Vandenberghe, *Convex Optimization*. New York, NY, USA: Cambridge University Press, 2004.

[42] B. H. Korte and J. Vygen, *Combinatorial optimization : theory and algorithms*, ser. Algorithms and combinatorics. Berlin, Heidelberg, Paris: Springer, 2000. [Online]. Available: http://opac.inria.fr/record=b1098131

[43] A. Hoffman and J. Kruskal, "Integral boundary points of convex polyhedra, in Linear Inequalities and Related Systems(H. Kuhn and A. Tucker, Eds.)," *Annals of Maths. Study*, vol. 38, pp. 223–246, 1956.

[44] J. Matousek and B. Gärtner, *Understanding and Using Linear Programming*, ser. Universitext. Springer Berlin Heidelberg, 2006. [Online]. Available: https://books.google.be/books?id=K8RHOmiIG8YC

[45] J. C. Nash, "The (dantzig) simplex method for linear programming," in *Computing in Science and Engg.* IEEE Educational Activities Department, 2000, vol. 2, no. 1, pp. 29–31.

[46] M. H. WRIGHT, "The interior-point revolution in optimization:history, recent developments, and lasting consequences," *AMERICAN MATHEMATICAL SOCIETY*, vol. 42, no. 1, p. 3956, Sep 2004.

[47] N. Karmarkar, "A new polynomial-time algorithm for linear programming," in *Proceedings of the Sixteenth Annual ACM Symposium on Theory of Computing*, ser. STOC '84. New York, NY, USA: ACM, 1984, pp. 302–311. [Online]. Available: http://doi.acm.org/10.1145/800057.808695

[48] J. Gondzio, "Interior point methods 25 years later," *European Journal of Operational Research*, p. 2012.

[49] S. Sra, S. Nowozin, and S. Wright, *Optimization for Machine Learning*, ser. Neural information processing series. MIT Press, 2012. [Online]. Available: https://books.google.be/books?id=JPQx7s2L1A8C

[50] R. Robere, "Interior point methods and linear programming," *University of Toronto*, 2012.

[51] "System simulation results on carrier aggregation for bursty traffic," 3GPP TSG-RAN WG1 MEETING #57, R1-091828, Tech. Rep.

[52] R. K. Jain, D.-M. W. Chiu, and W. R. Hawe, "A Quantitative Measure Of Fairness And Discrimination For Resource Allocation In Shared Computer Systems," DEC-TR-301, Digital Equipment Corporation, Tech. Rep., Sep. 1984. [Online]. Available: http://arxiv.org/abs/cs.NI/9809099

[53] K. Truemper, "A decomposition theory for matroids. v. testing of matrix total unimodularity," *Journal of Combinatorial Theory, Series B*, vol. 49, no. 2, pp. 241 – 281, 1990. [Online]. Available: http://www.sciencedirect.com/science/article/pii/0095895690900304

[54] J. Lee, *A First Course in Combinatorial Optimization*. Cambridge Texts in Applied Mathematics, 2004.